Structural Engineering and Mechanics, Vol. 4, No. 4 (1996) 383-396
DOI: http://dx.doi.org/10.12989/sem.1996.4.4.383

Buckling behaviour of plates partially restrained against rotation under stress gradient

Osama K. Bedair

Department of Civil Engineering, Concordia University, 1455 de Maisonneuve Blvd. W., Montreal, Quebec, H3G 1M8, Canada

Abstract. In this paper, the behavior of plates partially restrained against rotation under stress gradient is investigated. As a first stage, an energy formulation is presented to model this boundary condition and a general expression is derived for the prediction of the elastic buckling of the plate under this general loading condition. The accuracy of the derived expression is compared numerically using the Galerkin method with other available data for the two limiting conditions of rotationally free and clamped boundaries. Results show that the prediction is within a 5% difference.

The influence of rotational restraint and stress gradient upon the buckling load and the associated buckling mode is investigated. Numerical results show sensitivity of the buckling mode to the degree of rotational restraint and the variation of the buckling load with the stress gradient.

Key words: plate buckling; stiffened plate; plates under compression and bending; plates partially restrained against rotation; plate modelling using the energy method.

1. Introduction

Plates under compressive stress gradient can be encountered in the webs of beam-columns when subjected to axial compression and bending about the major axis or in stiffened box-girders. The flanges in the former and the stiffeners in the latter restrain both rotation and in-plane translation of the plate. The problem can be analyzed by invoking well established numerical methods (e.g., finite strip, finite element, finite difference, ··· etc.) where extensive computation cost and effort cannot be avoided; furthermore, closed form solutions may not be always possible. The objectives of this paper are to furnish this class of stability problems with closed form solutions and to investigate the influence of the rotational restraint and stress gradient on the buckling behaviour of the plate. A closed form solutions will be proposed that for design purposes, is suitable for hand-calculations.

Schuette and McCulloch (1947), Johnson and Noel (1953), investigated the buckling of infinitely long flat plates subject to pure in-plane bending. The plate was considered to be simply supported along the tension edge and rotationally restrained along the compression edge. To further simplify the analysis, a sinusoidal rotational restraint distribution was assumed at the compression edge. Walker (1966), (1967), (1968) investigated the local stability of the flanges and webs of initially perfect channel section under eccentric loading along the axis of symmetry. He used the Galerkin method of investigate numerically the buckling and post-buckling behaviour. A sinusoidal function was used to approximate the longitudinal out of plane deflection and a polynomial function

to approximate the transverse deflection. Rhodes, Harvey and Fok (1975), Rhodes and Harvey (1976), (1977) used the Ritz method to analyze plates with linearly varying displacement in the transverse direction. Usami (1982) employed the energy method to investigate the post-buckling behaviour of a simply supported plate in combined compression and bending. A sinusoidal function was used to approximate the out-of plane deflection and the resulting system of non-linear equations was solved numerically using the Newton-Raphson method. Lau and Hancock (1986) and Bradford (1989) presented a finite strip formulation for plates in combined bending and compression.

In this paper, the buckling behaviour of plates partially restrained against rotation under in-plane stress gradient is investigated. Closed form expression for predicting the buckling load under this loading condition is proposed. The accuracy of the derived expression is compared for two limiting conditions, rotationally free and rotationally clamped. The influence of the rotational restraint and the stress gradient coefficient upon the buckling stress is also investigated.

2. Theoretical analysis

Consider the plate of Fig. 1, supported along the unloaded edges, $y=\pm b/2$, by two flanges. Each flange has a cross sectional area (A_s), out of plane bending rigidity (I_y), in-plane bending rigidity (I_z) and torsional stiffness (C). This may represent the web of an I-section or a single panel of a stiffened plate. The plate is subjected to a linearly varying compressive load distribution, N_x, at its mid-plane given by

$$N_x=N_1\left[(1-\Psi)\eta+\frac{1}{2}(1+\Psi)\right] \tag{1}$$

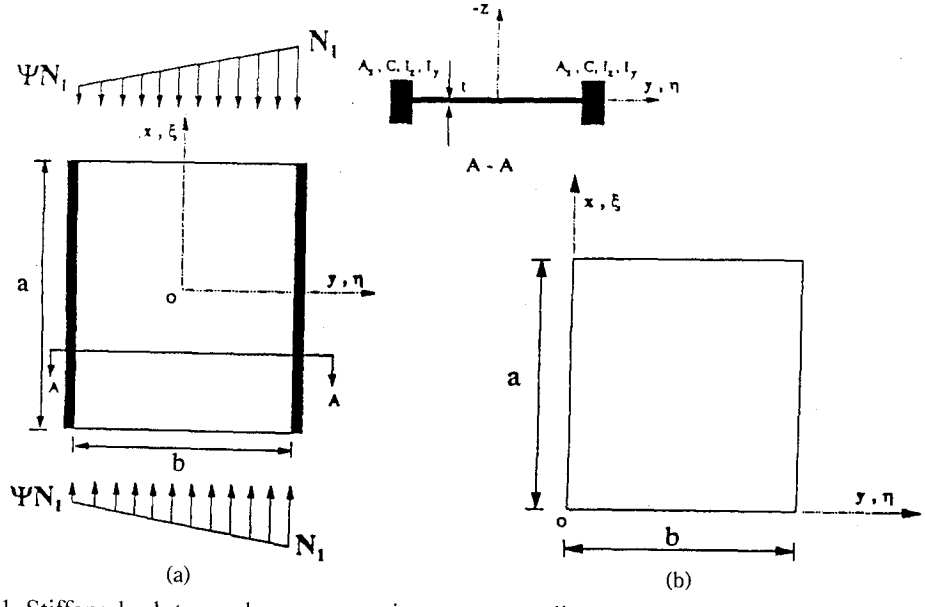

Fig. 1 Stiffened plate under compressive stress gradients (1a); Coordinate system for Galerkin's formulation (1b).

where $\eta=y/b$ and Ψ is defined as the stress gradient coefficient. When $\Psi=-1$ the plate is under pure in-plane bending and when $\Psi=1$, the plate is under uniform compression.

The buckling analysis of a plate, partially restrained against rotation along the unloaded edges, can be achieved by assuming the out-of plane deflection is described by three displacement functions as:

$$w=\{f_1 G_1(\eta)+f_2 G_2(\eta)\} F(\xi) \tag{2}$$

where $G_1(\eta)$ and $G_2(\eta)$ describe the transverse displacement profile and $F(\xi)$ describe the longitudinal displacement profile. ξ and η are non-dimensional parameters given by $\xi=x/a$ and $\eta=y/b$. It is further assumed that the transverse edges can be either simply supported or clamped.

Therefore, $F(\xi)$ at $\xi=\pm 1/2$ satisfies either of

$$F(\xi)=0, \qquad \frac{\partial^2 F(\xi)}{\partial \xi^2}=0 \tag{3}$$

or

$$F(\xi)=0, \qquad \frac{\partial F(\xi)}{\partial \xi}=0 \tag{4}$$

Furthermore $G_1(\eta)$ and $G_2(\eta)$ at $\eta=\pm 1/2$ should also satisfy

$$G_1(\eta)=0, \qquad \frac{\partial G_1(\eta)}{\partial \eta}=0 \tag{5}$$

and

$$G_2(\eta)=0, \qquad \frac{\partial^2 G_2(\eta)}{\partial \eta^2}=0 \tag{6}$$

Therefore, w satisfies the free rotation condition along the unloaded edges by setting $f_1=0$ and the rotationally clamped condition by setting $f_2=0$ in Eq. (2). The out of plane boundary conditions at $\eta=\pm 1/2$ are given by

$$w=0 \tag{7}$$

$$\left(\frac{\partial^2 w}{\partial \eta^2}+\frac{\nu}{\beta^2}\frac{\partial^2 w}{\partial \xi^2}=\Gamma\frac{\partial w}{\partial \eta}\right)_{\eta=\pm 1/2} \tag{8}$$

where β is the plate aspect ratio, Γ is a non-dimensional parameter referred to as the rotational restraint coefficient that depends upon the torsional stiffness, C, of the flanges and the plate bending rigidity per unit width, $D=Et^3/12(1-\nu^2)$, and ν is Poisson's ratio. It varies from 0 (rotationally free condition) to ∞ (rotationally clamped condition). Substituting Eq. (2) into Eq. (8) and using Eqs. (3)-(6), yields

$$\Gamma=\left(f_1\left\{\frac{\partial^2 G_1(\eta)}{\partial \eta^2}\right\}/f_2\left\{\frac{\partial G_2(\eta)}{\partial \eta}\right\}\right)_{\eta=\pm 1/2} \tag{9}$$

Substituting Eq. (9) into (2), w can be expressed in terms of Γ and either of f_1 or f_2, i.e.,

$$w=f_2\left\{\Gamma\left[\frac{\partial G_2(\eta)}{\partial \eta}\left(\frac{\partial^2 G_1(\eta)}{\partial \eta^2}\right)^{-1}\right]_{\eta=1/2} G_1(\eta)+G_2(\eta)\right\} F(\xi) \tag{10}$$

The total strain energy, Π, stored in the system is composed of U_1, the strain energy of bending of the plate, U_2 the strain energy in the restraining media, and T the potential energy of the applied load i.e.,

$$\Pi = U_1+U_2+T \tag{11}$$

Where U_1, U_2 and T are expressed in non-dimensional form as

$$U_1=\frac{D}{2\beta a^2}\int_{-1/2}^{1/2}\int_{-1/2}^{1/2}\left\{\left[\frac{\partial^2 w}{\partial \xi^2}+\beta^2\frac{\partial^2 w}{\partial \eta^2}\right]^2+2(1-\nu)\beta^2\left[\frac{\partial^2 w}{\partial \xi^2}\frac{\partial^2 w}{\partial \eta^2}-\left(\frac{\partial^2 w}{\partial \xi \partial \eta}\right)^2\right]\right\} d\xi\, d\eta \tag{12}$$

$$U_2=\frac{\beta C}{2b}f_2^2\int_{-1/2}^{1/2}\left[\left(\frac{\partial w}{\partial \eta}\right)^2_{\eta=1/2}+\left(\frac{\partial w}{\partial \eta}\right)^2_{\eta=-1/2}\right] F^2(\xi)\, d\xi \tag{13}$$

$$T=\frac{N_x}{2\beta}\int_{-1/2}^{1/2}\int_{-1/2}^{1/2}\left(\frac{\partial w}{\partial \xi}\right)^2 d\xi d\eta \tag{14}$$

Substituting Eq. (10) into (12), (13) and (14) yields

$$U_1=\frac{D}{2\beta a^2}f_2^2\int_{-1/2}^{1/2}\int_{-1/2}^{1/2}\left[\chi(\eta)\frac{\partial^2 F(\xi)}{\partial \xi}+\beta^2\frac{\partial^2 \chi(\eta)}{\partial \eta^2}F(\xi)\right]^2 d\xi\, d\eta \tag{15}$$

$$U_2=\frac{C}{2ab^2}f_2^2\int_{-1/2}^{1/2}\left[\left(\frac{\partial G_2(\eta)}{\partial \eta}\right)^2_{\eta=1/2}+\left(\frac{\partial G_2(\eta)}{\partial \eta}\right)^2_{\eta=-1/2}\right]\left[\frac{\partial F(\xi)}{\partial \xi}\right]^2 d\xi \tag{16}$$

$$T=\frac{N_1}{2\beta}f_2^2\int_{-1/2}^{1/2}\int_{-1/2}^{1/2}\left[\left(\frac{\partial F(\xi)}{\partial \xi}\right)^2\chi^2(\eta)\right]\left[(1-\Psi)\eta+\frac{1}{2}(1+\Psi)\right] d\xi\, d\eta \tag{17}$$

where

$$\chi(\eta)=\left\{\Gamma\left[\frac{\partial G_2(\eta)}{\partial \eta}\left(\frac{\partial^2 G_1(\eta)}{\partial \eta^2}\right)^{-1}\right]_{\eta=1/2} G_1(\eta)+G_2(\eta)\right\} \tag{18}$$

The critical load is therefore computed by minimizing Π with respect to f_2 to obtain

$$N_{cr}=K\frac{\pi^2 D}{b^2} \tag{19}$$

where K is given by

$$K=\frac{\int_{-1/2}^{1/2}\int_{-1/2}^{1/2}\left[\chi(\eta)\frac{\partial^2 F}{\partial\xi^2}+\beta^2\frac{\partial^2\chi}{\partial\eta^2}F(\xi)\right]^2 d\xi d\eta+\frac{Cb}{a^2D}\beta^4\int_{-1/2}^{1/2}\left[\left\{\left(\frac{\partial G_2(\eta)}{\partial\eta}\right)^2_{\eta=+1/2}+\left(\frac{\partial G_2(\eta)}{\partial\eta}\right)^2_{\eta=-1/2}\right\}\left(\frac{\partial F(\xi)}{\partial\xi}\right)^2\right]d\xi}{\pi^2\beta^2\int_{-1/2}^{1/2}\int_{-1/2}^{1/2}\left[\left(\frac{\partial F(\xi)}{\partial\xi}\right)^2\chi^2(\eta)\right]\left[(1-\Psi)\eta+\frac{1}{2}(1+\Psi)\right]d\xi d\eta} \tag{20}$$

3. Results and discussion

In this section, results are obtained to show the sensitivity of the buckling load and corresponding buckling mode to the rotational restraint coefficient, Γ, and the stress gradient parameter, Ψ. The functions $G_1(\eta)$, $G_2(\eta)$ and $F(\xi)$ of Eq. (2) are chosen, for $\Psi\geq 0$, to be

$$G_1(\eta)=4\left(\eta^2+\frac{\cos(\eta\pi)}{\pi}\right)-1 \tag{21}$$

$$G_2(\eta)=\cos(\eta\pi) \tag{22}$$

$$F(\xi)=\cos(m\pi\xi) \qquad (m=1,\ 3,\ 5,\ \cdots) \tag{23}$$

$$=\sin(m\pi\xi) \qquad (m=2,\ 4,\ 6,\ \cdots) \tag{24}$$

indicating that the plate is simply supported along the loaded edges and elastically restrained against rotation along the unloaded edges. Analogous results can be obtained for clamped-clamped loaded edges by choosing a suitable displacement function, $F(\xi)$, satisfying Eq. (4) Substituting the displacement functions described by Eqs. (21)-(24) into Eq. (20) the following expression for the buckling load factor, K, is obtained

$$K=2\left\{\frac{[0.00921\,\kappa^2+0.04736\,\kappa^{-2}+0.02276]\,\Gamma^2+[0.18943\,\kappa^2+0.59472\,\kappa^{-2}+0.37886]\,\Gamma+[\kappa+\kappa^{-1}]^2}{[0.00921\,\Gamma^2+0.18943\,\Gamma+1]\ [1+\Psi]}\right\} \tag{25}$$

where $\kappa=m/\beta$, m is the number of half-wave length in the longitudinal direction, β is the plate aspect ratio$=a/b$, $\Gamma=(\pi^2GJ/Db)(b/\lambda)^2$, G and J are the shear modulus and the torsional rigidity of the stiffeners, D and b are the flexural rigidity and width of the plate and λ is half wave length$=a/m$. Note that the restriction stipulated on $F(\xi)$ by Eqs. (23) and (24) for even and odd values of m to satisfy Eq. (3) due to the coordinate system chosen does not affect the form of K owing to the following integral property

$$\int_{-1/2}^{1/2}\sin^2(m\pi\xi)\ d\xi=\int_{-1/2}^{1/2}\cos^2(m\pi\xi)\ d\xi=1/2 \tag{26}$$

3.1. Numerical verification

In this section the accuracy of the derived buckling coefficient from Eq. (25) is examined numerically using the Galerkin method for the two limiting conditions of rotationally free, i.e.

simply supported ($\Gamma=0$), and rotationally clamped, ($\Gamma\to\infty$). For convenience in mathematical manipulation, the origin of the plate is shifted to the lower left hand corner as shown in Fig. 1(b).

The differential equation governing the behaviour of the plate subject to a stress gradient in the transverse direction is given, in non-dimensional form, as

$$\frac{\partial^4 w}{\partial \xi^4}+2\beta^2\ \frac{\partial^4 w}{\partial \xi^2 \partial \eta^2}+\beta^4\ \frac{\partial^4 w}{\partial \eta^4}=\frac{a^2}{D}\ N_x\left(\frac{\partial^2 w}{\partial \xi^2}\right) \tag{27}$$

The Galerkin method after substituting the expression $w(\xi,\eta)$ that satisfies the kinematic boundary condition leads to the following eigenvalue problem

$$\sum_{m=1}^{N}\sum_{n=1}^{N}\sum_{i=1}^{N}\sum_{j=1}^{N}|Q_{mnij}-\lambda R_{mnij}|\ A_{mnij}=0 \tag{28}$$

The matrices Q_{mnij} and R_{mnij} are each of order $(m\times n)\times(i\times j)$ and the magnitudes of their entries depends upon the form of $w(\xi,\eta)$ selected and $\lambda=N_1 b^2/\pi^2 D$. For the rotationally free condition, the out of plane displacement function is assumed to be

$$w(\xi,\eta)=\sum_{m=1}^{N}\sum_{n=1}^{N}\ \sin(m\pi\xi)\ \sin(n\pi\eta) \tag{29}$$

The entries of Q_{mnij} and R_{mnij} of the eigen-problem of Eq. (28) become

$$[Q_{mnij}]_{mxn}=\frac{1}{4}\left(\frac{m^2}{\beta}+\beta\ n^2\right)^2\ \delta_{mi}\ \delta_{nj},\ [R_{mnij}]_{mxn}=m^2[\Psi\ K_{mnij}+(1-\Psi)\ I_{mnij}] \tag{30}$$

where

$$[K_{mnij}]_{mxn}=\frac{1}{4}\ \delta_{mi}\ \delta_{nj} \tag{31}$$

$$[I_{mnij}]_{mxn}=\frac{\delta_{mi}\ \delta_{nj}}{8} \tag{32}$$

$$=-\frac{2}{\pi^2}\frac{nj}{(j^2-n^2)^2}\ \delta_{mi}\qquad \textit{if } n+j \textit{ is odd, } =0 \textit{ elsewhere} \tag{33}$$

where δ_{mi} is the kronecker delta defined as $\delta_{mi}=1$ if $m=i$ and zero otherwise. A computer program was developed to generate and solve the above eigenvalue problem. Experience has shown that convergence of the truncated series defined by Eq. (29) can be attained with reasonable accuracy using 4 or 5 terms. The difference is less than 1% from the analytical values for $\Psi=1$ and various β values.

The upper part of Table 1 shows a comparison between the buckling factor, K, obtained from the analytical expression Eq. (25) and the Galerkin method. The value of K is obtained

Table 1 Comparison of K from Eqs. (34), (39) and the Galerkin method

(a) Rotationally free condition

β	Ψ	Present	Galerkin	Difference (%)
1	0	8	7.84	2.04
	0.5	5.33	5.32	0.19
	1	4	4	0
1.5	0	8.68	8.42	3.1
	0.5	5.78	5.70	1.4
	1	4.34	4.35	1
2	0	8	7.84	2.04
	0.5	5.33	5.32	0.19
	1	4	4	0

(b) Rotationally clamped condition

1	0	15.51	15.45	0.4
	0.25	12.41	12.36	0.4
	0.5	10.34	10.30	0.4
	0.75	8.86	8.83	0.34
	1	7.75	7.72	0.39
2	0	14.01	13.98	0.21
	0.25	11.21	11.18	0.27
	0.5	9.34	9.32	0.21
	0.75	8.01	7.99	0.25
	1	7.01	6.99	0.28

by setting $\Gamma=0$ in Eq. (25) which reduces to the following expression

$$K=2\left[\frac{(\kappa+\kappa^{-1})^2}{1+\Psi}\right] \tag{34}$$

The Galerkin solution was based on nine terms of the displacement series. As can be seen from the table, the difference fluctuates from 0% to 3.1% reflecting the high accuracy of Eq. (34). It should be mentioned that the buckling modes were identical for both cases.

For the rotationally clamped condition, a kinematically admissible displacement function satisfying the zero deflection and slope conditions can be assumed as

$$w(\xi,\eta)=\sum_{m=1}^{N}\sum_{n=1}^{N}\sin(m\pi\xi)\ \sin^2(n\pi\eta) \tag{35}$$

The entries of Q_{mnij} and R_{mnij} of Eq. (28) in this case are given by

$$[Q_{mnij}]_{m\times n}=\left[\frac{m^4}{\beta^2}\ \theta_{nj}+(m^2n^2+2n^4\beta^2)\ \delta_{nj}\right]\frac{\delta_{mi}}{2} \tag{36}$$

$$[R_{mnij}]_{mxn} = m^2 \ \theta_{nj} \ (1+\Psi) \ \frac{\delta_{mi}}{4} \tag{37}$$

where θ_{nj} is given by

$$\theta_{nj} = \frac{3}{8} \ \delta_{nj}, \ = \frac{1}{4} \ \text{if} \ n \neq j \tag{38}$$

The numerical solution was based on nine terms of the series and the analytical values were computed from Eq. (25) for $\Gamma \to \infty$, i.e.

$$K \to \frac{2 \ \kappa^2 + 10.284 \ \kappa^{-2} + 4.943}{[1+\Psi]} \quad \text{as} \ \Gamma \to \infty \tag{39}$$

The lower part of Table 1 shows a comparison between the predictions of the analytical expression Eq. (39) and the numerical values using the Galerkin method for $\beta = 1$ and 2 and $\Psi = 0$, 0.25, 0.5, 0.75 and 1 for the rotationally clamped condition. It can be seen that both predictions are in excellent agreement.

3.2. Comparison with existing formulas

A comparison is made between Eqs. (34) and (39) and various formulas and data for the limiting conditions of simply supported and clamped plates under stress gradients, available in standard stability references and structural handbooks. Note that Eq. (25) represents a more general case of plates partially restrained against rotation. Gaylord and Gaylord (1990) presented an approximate formula based on the German specification, DIN4114, given by

$$K = \frac{8.4}{1.1+\Psi} \qquad \text{for} \ \beta \geq 1 \tag{40}$$

$$K = \frac{2.1}{1.1+\Psi} \left(\beta + \frac{1}{\beta} \right)^2 \qquad \text{for} \ \beta \leq 1 \tag{41}$$

A comparison is made in Table 2 between Eq. (34) and Eq. (41); as can be seen the values are close to each other. It can also be observed that when the aspect ratio is not an integer, the difference between the two equations increases. This is because Eq. (41) is the asymptotic value of K, which can be obtained by substituting $\kappa = 1$ in Eq. (34) resulting in the following

$$K = \frac{8}{1+\Psi} \tag{42}$$

which is very close to Eq. (41). However, for $\beta = 1.5$ the buckling mode is two half sine waves, i.e. $m = 2$, and the theoretical value of K, of Eq. (34), is

Table 2 Comparison of K from Eqs. (34), (41) and (44)

β	Ψ	DIN 4114	Beedle	Present
1	1	4	4	4
	1/3	5.86	5.96	6
	1/2	5.25	5.32	5.33
	0	7.64	7.79	8
1.5	1	4	4	4.34
	1/3	5.86	5.96	6.51
	1/2	5.25	5.32	5.78
	0	7.64	7.79	8.68
2	1	4	4	4
	1/3	5.86	5.96	6
	1/2	5.25	5.32	5.33
	0	7.64	7.79	8

Table 3 Comparison of K presented by Galambos (1988) and Eqs. (34) and (39)

Ψ	Unloaded edges	Galambos	Present
0	Simply supported	7.8	8
	Clamped-clamped	13.6	14.01
1/3	Simply supported	5.8	6
	Clamped-clamped	–	10.5

$$K=\frac{8.68}{1+\Psi} \tag{43}$$

which explains the reason for a larger difference in this case. An alternative formulation based on the West European standards, presented by Beedle (1991), is given by

$$K=\frac{16}{\sqrt{(1+\Psi)^2+0.112(1-\Psi)^2}+(1+\Psi)} \tag{44}$$

Table 2 shows also a comparison between Eq. (44) and Eq. (34). It is seen that Eq. (44) gives a constant value independent of β, similar to Eq. (41), leading, again, to larger differences for $\beta=1.5$ as explained earlier.

Limited data was available for comparison of the clamped limiting condition. Galambos (1988) presented some numerical values for this condition for long plates. Comparative data is shown in Table 3 in which the K factor of Eq. (39) for long plates becomes asymptotic to $14.01/(1+\Psi)$.

3.3. Elastically restrained condition

The previous section is concerned with the computation of the buckling load for plates either

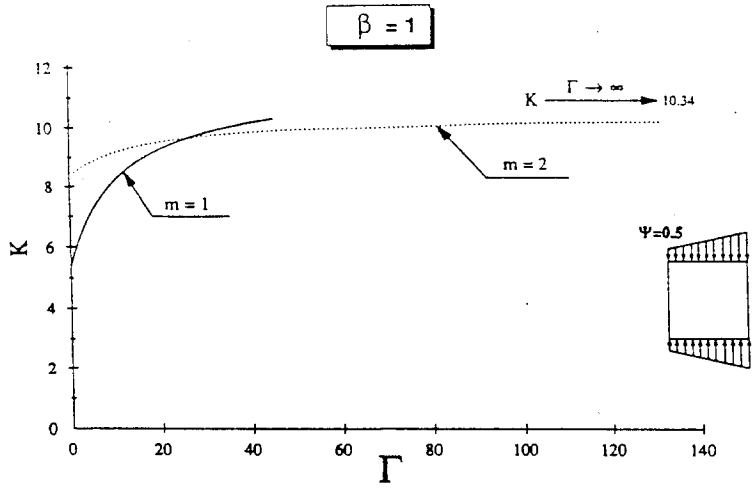

Fig. 2 Variation of K with Γ ($\beta=1$, $\Psi=0.5$).

simply supported or clamped along the unloaded edges. The former assumes the flanges have zero torsional stiffness while the latter assumes an infinite value. In reality, the flanges have finite rotation capacity and thus the plate is partially restrained against rotation along those edges. In this section typical results are given detailing the buckling behaviour and showing the transition from the simply supported to the rotationally clamped condition for various aspect ratios, β, and stress gradient coefficient, Ψ.

Fig. 2 shows the transition of the buckling load factor, K, from the simply supported to the clamped condition for stress gradient coefficient, $\Psi=0.5$ and aspect ratio, $\beta=1$. The solid curve represents K values for a buckling mode of one-half sine wave, $m=1$, and the dotted curve for a full sine wave buckling mode, i.e., $m=2$. Starting with the simply supported condition, i.e., $\Gamma=0$, the plate buckles in one-half sine wave with $K=5.33$; the value of K then increases with increasing Γ until the asymptotic value to the rotationally clamped condition, $K\rightarrow 10.34$, is attained as $\Gamma\rightarrow\infty$. During this interval the plate buckling mode changes from a one-half sine wave to a full sine wave, corresponding to the buckling mode of square clamped plates. The changes from $m=1$ to $m=2$, in this case, occurs at $K\approx 9.65$. The curve also shows rapid initial increases in K for small values of Γ. The asymptotic value of K is visible at $\Gamma\approx 50$. Fig. 3 also shows the variation of K with Γ for $\beta=2$ and $\Psi=0.2$. The plate buckling mode in this case changes from a full sine wave, $m=2$, to three half, $m=3$, sine waves over $\Gamma=0$ to ∞ and the K value at this transition point in 8.9.

Figs. 4-6 show the variation of K with stress gradient Ψ, from the triangular load pattern, $\Psi=0$, to uniform compression, $\Psi=1$, for $\Gamma=0$, 5, 10, 20, 50, 100 and ∞ and representative $\beta=1$, 4, 8. The numbers in brackets in the legend box refer to the buckling mode, m, for each Γ. Based on a study of several plate aspect ratios, it was found that, as the plate gets longer, the buckling mode becomes very sensitive in the early stages to slight increases of rotational restraint, Γ. This can be observed for the representative cases of $\beta=1$, 4 and 8. For $\beta=8$, the number of half sine-waves changes from $m=8$ to 9 to 10 within $\Gamma=0$-5, whereas, for $\beta=4$ the plate changes the buckling mode only once, $m=4$ to 5, within this interval of Γ. For $\beta=1$, the buckling mode does not change over a much larger range. The difference in K for the

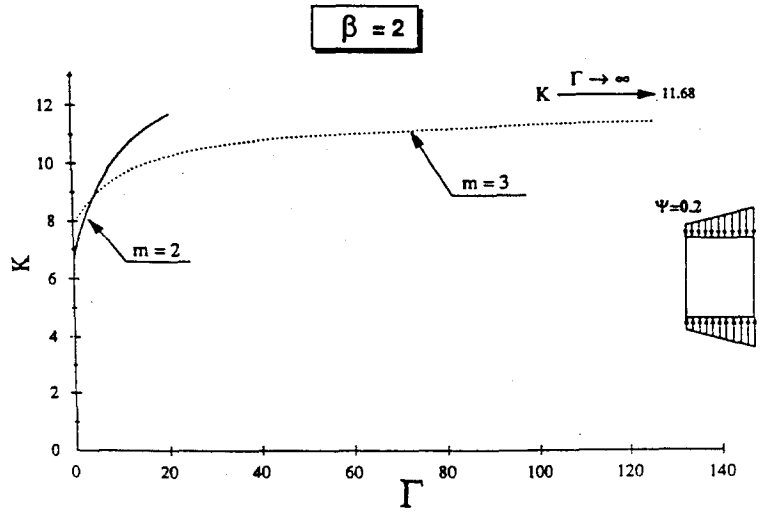

Fig. 3 Variation of K with Γ ($\beta=2$, $\Psi=0.2$).

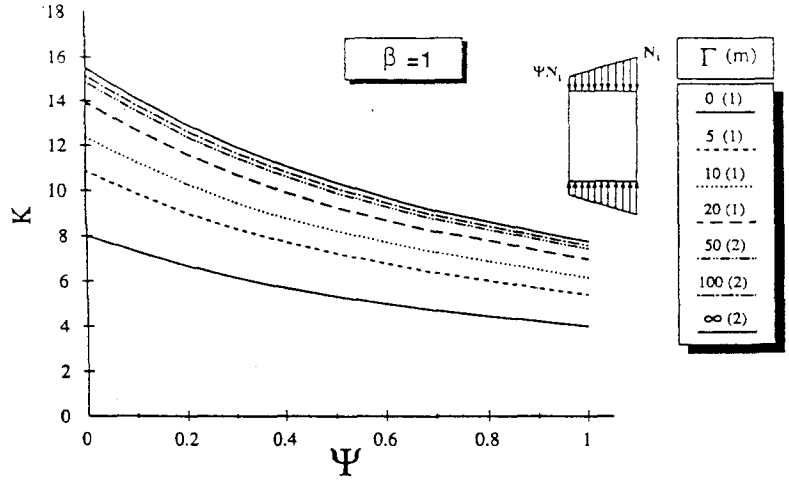

Fig. 4 Variation of K with stress gradient coefficient Ψ ($\beta=1$, Γ is variable).

rotationally free condition, $\Gamma=0$ and the rotationally clamped condition, $\Gamma\to\infty$, increases as Ψ decreases. For example, for $\beta=1$, the difference between these two limiting condition is 3.76 for $\Psi=1$ whereas for $\Psi=0$ the difference increases to 7.51.

4. Conclusions

The paper presents an analytical formulation for the determination of the buckling load and the associated buckling mode of plate partially restrained against rotation and under in-plane stress gradients. Unlike the classical assumption where the plate and the attached flanges are assumed to be hinged along their junction, the flanges are assumed to posses a finite rotation

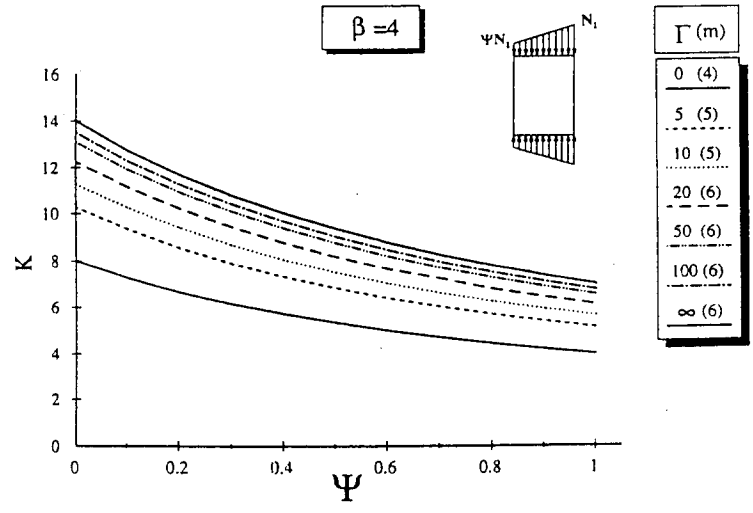

Fig. 5 Variation of K with stress gradient coefficient Ψ ($\beta=4$, Γ is variable).

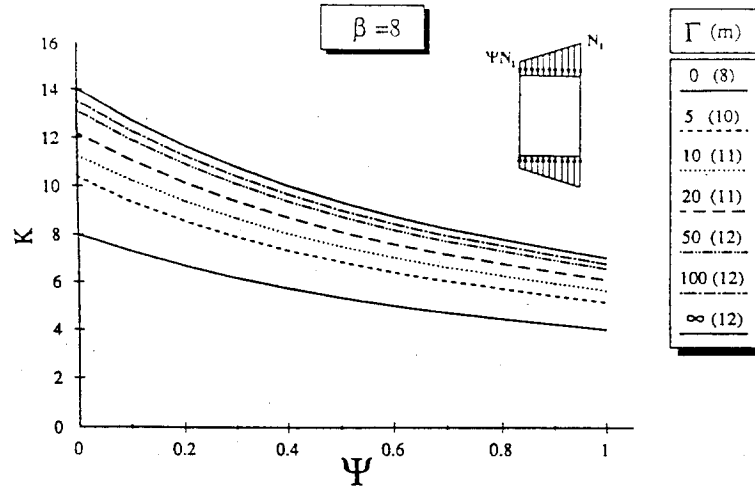

Fig. 6 Variation of K with stress gradient coefficient Ψ ($\beta=8$, Γ is variable).

capacity. Using the energy method, approximate explicit expressions are derived for the buckling coefficient. These expressions are verified numerically using the Galerkin method and compared with existing data available for the two extreme conditions of rotationally free and clamped boundaries.

The paper also investigates the influence of rotational restraint and stress gradient upon the associated buckling mode. Numerical results show that changes of the buckling mode occur with increases in the rotation restraint coefficient. With knowledge about the buckling behaviour of the plate, the post-buckling behaviour can now assessed.

Acknowlegements

The financial support provided by the Natural Sciences and Engineering Research Council of Canada (NSERC) to the author is gratefully acknowledged.

References

Bedair, O.K. and Sherbourne, A.N. (1993), "Plate/stiffener assemblies in uniform axial compression: Part I-Buckling analysis", *J. Engrg. Mech., ASCE*, **119**, 1937-1955.

Beedle, L.S. (1991), *Stability of Metal Structures, a World View*, 2nd ed., Structureal Stability Research Council, USA.

Bradford, M.A. (1989), "Buckling of longitudinally stiffened plates in bending and compression", *Can J. Civ. Eng.*, **16**, 607-614.

Column Research Committee of Japan (1971), *Handbook of Structural Stability*, Corona Publishing Co., Tokyo.

Galambos, T.V. (1988), *Guide to Stability Design Driteria for Metal Structures*, 4th ed., Structural Stability Research Council, John Wiley & Sons, New York.

Gaylord, E.H. and Gaylord, C.N. (1990), *Structural Engineering Handbook*, McGraw-Hill, USA.

Johnson, J.H. and Noel, G.R. (1953), "Critical bending stress of flat rectangular plates supported along all edges and elastically restrained against rotation along the unloaded compression edge", *J. Aero. Sci.*, **19**, 535-540.

Lau, S.C.W. and Hancock, G.J. (1986), "Buckling of thin flat-walled structures by a spline finite strip method", *Thin Walled Structures*, **4**, 269-294.

Loughlan, J. (1983), "The ultimate load Ssensitivity of lipped channel columns to column axis imperfection", *Thin Walled Structures*, **1**, 75-96.

Rhodes, J. and Harvey, J.M. (1977), "Examination of plate post-buckling behaviour", *J. Engrg. Mech., ASCE*, **103**, 461-478.

Rhodes, J. and Harvey, J.M. (1976), "Plain channel section struts in compression and bending beyond the local buckling load", *Int. J. Mech. Sci.*, **8**, 511-519.

Rhodes, J., Harvey, J.M. and Fok, W.C. (1975), "The load carrying capacity of initially imperfect eccentrically loaded plates", *Int. J. Mech. Sci.*, **17**, 161-175.

Schuette, E.H. and McCulloch, J.C. (1947), "Charts for the minimum weight design of multiweb wings in bending", *NACA TN* 1323.

Sherbourne, A.N. and Bedair, O.K. (1993), "Plate/stiffener assemblies in uniform axial compression: Part II-Post-buckling analysis", *J. Engrg. Mech., ASCE*, **119**, 1956-1972.

Timoshenko, S.P. and Gere, J.M. (1961), *Theory of Elastic Stability*, McGraw-Hill.

Usami, T. (1982), "Post-buckling of plates in compression and bending", *ASCE ST3*, **108**, 591-609.

Walker, A.C. (1968), "Maximum loads for eccentrically loaded thin-walled channel struts", *IABSE*, **28**, 169-181.

Walker, A.C. (1967), "Flat rectangular plates subjected to a linearly-varying edge compressive loading", *Thin Walled Structures*, A.H. Chilver, ed., Catto & Windus, England, 208-247.

Walker, A.C. (1966), "Local instability in plates and channel struts", *ASCE*, **92**, 39-55.

Notations

a	length of the plate
A	cross sectional area of the stiffeners

b	width of the plate
C	torsional rigidity of the stiffeners
D	plate bending rigidity per unit width, $=E\ t^3/12\ (1-\nu^2)$
E	elastic modulus
f_1, f_2	amplitudes of the displacement functions
$F(\xi)$	function that describe the longitudinal displacement profile
$G_1(\eta)$, $G_2(\eta)$	functions that describe the transverse displacement profile
I_y, I_z	out of plane and in-plane bending rigidity of the stiffeners
K	buckling coefficient
m	number of half waves in the longitudinal direction
N_x	compressive forces per unit length in the x direction
N_{cr}	buckling load per unit length
t	thickness of the plate
β	plate aspect ratio
Γ	torsional restraint coefficient
η	nondimensional width, $=y/b$
ν	Poisson ratio
ξ	nondimensional length, $=x/a$; and
Π	total strain energy of the plate and the attached stiffeners
Ψ	stress gradient coefficient
$\lambda_{\sim}$	eigen-vector
λ	half-wave length $=a/m$